

Higgs Boson Flavor-Changing Neutral Decays into Bottom Quarks in Supersymmetry

Santi Béjar ^a, Francesc Dilmé ^b, Jaume Guasch ^c, Joan Solà ^{b,d}

^a *Grup de Física Teòrica and IFAE, Universitat Autònoma de Barcelona, E-08193, Bellaterra, Barcelona, Catalonia, Spain*

^b *Dep. Estructura i Constituents de la Matèria, Universitat de Barcelona, Diagonal 647, E-08028, Barcelona, Catalonia, Spain*

^c *Theory Group LTP, Paul Scherrer Institut, CH-5232 Villigen PSI, Switzerland*

^d *C.E.R. for Astrophysics, Particle Physics and Cosmology **

ABSTRACT: We analyze the maximum branching ratios for the Flavor Changing Neutral Current (FCNC) decays of the neutral Higgs bosons of the Minimal Supersymmetric Standard Model (MSSM) into bottom quarks, $h \rightarrow b\bar{s}$ ($h = h^0, H^0, A^0$). We consistently correlate these decays with the radiative B-meson decays ($b \rightarrow s\gamma$). A full-fledged combined numerical analysis is performed of these high-energy and low-energy FCNC decay modes in the MSSM parameter space. Our calculation shows that the available data on $B(b \rightarrow s\gamma)$ severely restricts the allowed values of $B(h \rightarrow b\bar{s})$. While the latter could reach a few percent level in fine-tuned scenarios, the requirement of naturalness reduces these FCNC rates into the modest range $B(h \rightarrow b\bar{s}) \sim 10^{-4} - 10^{-3}$. We find that the bulk of the MSSM contribution to $B(h \rightarrow b\bar{s})$ could originate from the strong supersymmetric sector. The maximum value of the FCNC rates obtained in this paper disagree significantly with recent (over-)estimates existing in the literature. Our results are still encouraging because they show that the FCNC modes $h \rightarrow b\bar{s}$ can be competitive with other Higgs boson signatures and could play a helpful complementary role to identify the supersymmetric Higgs bosons, particularly the lightest CP-even state in the critical LHC mass region $m_{h^0} \simeq 90 - 130$ GeV.

KEYWORDS: Higgs Physics, Supersymmetry Phenomenology, Rare Decays.

*Associated with Instituto de Ciencias del Espacio-CSIC.

1. Introduction

Experimentally, processes involving Flavor Changing Neutral Current (FCNC) have been shown to have extremely low rates [1]. Theoretically, their rareness can be explained by the GIM mechanism [2], which is related to the unitarity of the mixing matrices between quarks. The Minimal Standard Model (SM) embeds naturally the GIM mechanism, due to the presence of only one Higgs doublet giving mass simultaneously to the down-type and the up-type quarks, and as a result no tree-level FCNCs interactions appear. FCNCs are radiatively induced, and are therefore automatically small. The addition of further Higgs doublets to the SM in the most general way introduces tree-level FCNC interactions, which would predict significant FCNC rates. However, by introducing an *ad-hoc* discrete symmetry these interactions are forbidden. This gives rise to two classes of Two-Higgs-Doublet Models (2HDM) which avoid FCNCs at the tree-level, known conventionally as type I and type II 2HDMs [3].

Supersymmetry (SUSY) [4–7], on the other hand, provides an appealing extension of the SM, which unifies the fermionic and bosonic degrees of freedom of the fundamental particles, and provides a natural solution to the hierarchy problem. The search for SUSY particles has been one of the main programs of the past experiments in high energy physics (LEP, SLD, Tevatron), and continues to play a central role in the present accelerator experiments (Tevatron II), and in the planning of future experimental facilities, like the LHC and the LC [8–10]. The Minimal Supersymmetric Standard Model (MSSM) is the simplest extension of the SM which includes SUSY, and for this reason its testing will be one of the most prominent aims of these powerful experiments.

Complementary to direct searches, one can also look for effects of particles beyond the SM by studying their radiative effects. Much work along these lines has been made over the past two decades. FCNCs may play an important role here because they are essentially loop-induced. Hence SM and non-SM loops enter the FCNC observables at the same order of perturbation theory, and new physics competes on the same footing with SM physics to generate a non-vanishing value for these rare processes. It may well be that the non-SM effects are dominant and become manifest. Conversely, it may happen that they become highly constrained. The power of FCNC observables can be gauged e.g. by the implications of the bottom-quark rare decay $b \rightarrow s\gamma$: the experimentally measured allowed range $B(b \rightarrow s\gamma) = (3.3 \pm 0.4) \times 10^{-4}$ [1, 11–16] may impose tight constraints on extensions of the SM. For example, it implies a lower bound on the charged Higgs boson mass $m_{H^\pm} \gtrsim 350$ GeV in general type II 2HDMs [17–20].

The most general MSSM includes tree-level FCNCs among the extra predicted particles, which induce one-loop FCNC interactions among the SM particles. Given the observed smallness of these interactions, tree-level SUSY FCNCs are usually avoided by including one of the two following assumptions: either the SUSY particle masses are very large, and their radiative effects are suppressed by the large SUSY mass scale; or the soft SUSY-breaking squark mass matrices are aligned with the SM quark mass matrix, so that both mass matrices are simultaneously diagonal. However, if one looks closely, one soon realizes that the MSSM does not only include the possibility of tree-level FCNCs, but it actually *re-*

quires their existence [21]. Indeed, the requirement of $SU(2)_L$ gauge invariance means that the up-left-squark mass matrix can not be simultaneously diagonal to the down-left-squark mass matrix, and therefore these two matrices can not be simultaneously diagonal with the up-quark and the down-quark mass matrices, that is, unless both of them are proportional to the identity matrix. But even then we could not take such possibility too seriously, for the radiative corrections would produce non-zero elements in the non-diagonal part of the mass matrix. All in all, we naturally expect tree-level FCNC interactions mediated by the SUSY partners of the SM particles. The potentially largest FCNC interactions are those originating from the strong supersymmetric (SUSY-QCD) sector of the model (viz. those interactions involving the squark-quark-gluino couplings), and in this paper we mainly concentrate on them. These couplings induce FCNC loop effects on more conventional fermion-fermion interactions, like e.g. the gauge boson-quark vertices Vqq' .

Of course, low energy meson physics puts tight constraints on the possible value of the FCNC couplings, especially for the first and second generation squarks which are sensitive to the data on $K^0 - \bar{K}^0$ and $D^0 - \bar{D}^0$ [22, 23]. The third generation system is, in principle, much loosely constrained, since present data on $B^0 - \bar{B}^0$ mixing still leaves a large room for FCNCs, and the most stringent constraints are given by the $B(b \rightarrow s\gamma)$ measurement [11–16]. Therefore the relevant FCNC gluino coupling δ_{23} [22, 23] (see Section 3) is not severely bound at present. The lack of tight FCNC constraints in the top-bottom quark doublet enables the aforementioned lower bound on the charged Higgs boson mass in the MSSM to be easily avoided, to wit: by arranging that the SUSY-electroweak (SUSY-EW) contribution to $B(b \rightarrow s\gamma)$ from the top-squark/chargino loops screens partially the charged Higgs boson contribution. This situation can be naturally fulfilled if the higgsino mass parameter (μ) and the soft SUSY-breaking top-squark trilinear coupling (A_t) satisfy the relation $\mu A_t < 0$ [24–28].

The FCNC gluino interactions also induce large contributions to $B(b \rightarrow s\gamma)$. It should however be noted that the leading contributions to the Vqq' FCNC interactions from the third quark generation correspond to a *double insertion* term, in which the squarks propagating in the loop suffer a double mutation: a flavor conversion and a chirality transition. This fact has been demonstrated in the $B(b \rightarrow s\gamma)$ observable itself [29], as well as in the FCNC rare decay width $\Gamma(t \rightarrow cg)$ [30, 31]. As a consequence, the loose limits on the third generation FCNC interactions derived under the assumption that the leading terms contributing to $b \rightarrow s\gamma$ correspond to the *single particle insertion approximation* [22, 23] are not valid, and more complex expressions must be taken into account [32].

Concerning the FCNC interactions of Higgs bosons with third generation quarks, it was demonstrated long ago [30, 31] that the leading term corresponds to a *single particle insertion approximation*, which produces a flavor change in the internal squark loop propagator, since in this case the chirality change can already take place at the squark-squark-Higgs boson interaction vertex. Adding this to the fact that the Higgs bosons (in contrast to gauge bosons) have a privileged coupling to third generation quarks, one might expect that the FCNC interactions of the type quark-quark-Higgs bosons in the MSSM become highly strengthened with respect to the SM prediction. This was already proven in the rare decay channels $\Gamma(t \rightarrow ch)$ [30, 31] (h being any of the neutral Higgs bosons of

the MSSM $h \equiv h^0, H^0, A^0$), where the maximum rate of the SUSY-QCD induced branching ratio was found to be $BR(t \rightarrow ch) \simeq 10^{-5}$, eight orders of magnitude above the SM expectations $BR(t \rightarrow cH^{SM}) \simeq 10^{-13}$. Similar enhancement factors have been found in the top-quark-Higgs boson interactions in other extensions of the SM [31, 33, 34].

From the experience of the previous calculations with the top quark, we expect similar enhancements in the FCNC interactions of the MSSM Higgs bosons with the bottom quark. Indeed, the purpose of this paper is to quantify, in a reliable way, the MSSM expectations on the FCNC Higgs boson decay modes

$$h \rightarrow b\bar{s}, \quad h \rightarrow \bar{b}s \quad (h = h^0, H^0, A^0). \quad (1.1)$$

There are other FCNC decay modes involving light quarks. However, only these bottom quark channels are relevant, as the remaining FCNC decays into light quarks are negligible in the MSSM. Moreover, the FCNC decays of Higgs bosons into bottom quarks are specially interesting as they can provide an invaluable tool to discriminate among different extended Higgs boson scenarios in the difficult LHC range $90 < m_h < 130$ GeV [8, 9].

In this paper we present what we believe is the first realistic estimate of the SUSY-QCD contributions to the FCNC branching ratios of the MSSM Higgs bosons into bottom quark. Specifically, we compute

$$B(h \rightarrow q q') = \frac{\Gamma(h \rightarrow q q')}{\Gamma(h \rightarrow X)} \equiv \frac{\Gamma(h \rightarrow b\bar{s}) + \Gamma(h \rightarrow \bar{b}s)}{\sum_i \Gamma(h \rightarrow X_i)} \quad (1.2)$$

for the three Higgs bosons of the MSSM, $h = h^0, H^0, A^0$, where $\Gamma(h \rightarrow X)$ is the – consistently computed – total width in each case. The maximization process of the above branching ratios in the MSSM parameter space is performed on the basis of a simultaneous analysis of the relevant partial decay widths and of the branching ratio of the low-energy FCNC process $b \rightarrow s\gamma$, whose value is severely restricted by experiment [11–16]. It turns out that the maximum FCNC rates that we find disagree quite significantly with some simplified estimates that have recently appeared in the literature [35]. According to these authors the FCNC decay rate of some MSSM Higgs bosons into bottom quarks can reach the level $B(h \rightarrow q q') \sim 25\%$. We find this value untenable, even more given the fact that in Ref. [35] no attempt is made to verify the restrictions of the parameter space imposed by the low energy data on $B(b \rightarrow s\gamma)$.¹

The structure of the paper is as follows. In Section 2 we estimate the expected branching ratios and describe the structure of Eq. (1.2) in the MSSM in more detail; in Section 3 we present the numerical analysis, and in Section 4 we deliver our conclusions.

2. Partial widths and branching ratios

First of all let us estimate the branching ratio (1.2) in the SM. It is not necessary to perform a detailed calculation to suspect that it is rather small. Using dimensional analysis, power

¹See also Ref. [36] for a combined analysis of flavor-violating and CP-violating MSSM couplings.

counting, CKM matrix elements and dynamical features we expect that the maximum branching ratio of the SM Higgs boson H^{SM} into bottom quark is at most of order²

$$BR(H^{SM} \rightarrow b \bar{s}) \sim \left(\frac{|V_{ts}|}{16\pi^2} \right)^2 \alpha_W G_F \left(\frac{m_H^4}{m_b^2} \right) \lesssim 10^{-7} \quad (\text{if } m_H < 2 M_W). \quad (2.1)$$

Here G_F is Fermi's constant and $\alpha_W = g^2/4\pi$, g being the $SU(2)_L$ weak gauge coupling. This result should hold for a SM Higgs boson mass $m_H < 2 M_W$, and in particular in the critical LHC region $m_H \simeq 90 - 130$ GeV. We have approximated the loop form factor by just a constant prefactor, and the numerical value is an approximate upper bound assuming that we approach $m_H = 2 M_W$ from below. We have taken $V_{ts} = 0.04$ and $m_b = 5$ GeV for this estimate. In spite of the crudeness of the estimate, direct evaluation with programs FeynArts, FormCalc and LoopTools [37–39] confirms the order of magnitude (2.1)³. On the other hand, if $m_H > 2 M_W$, more specifically if $m_H > m_t$, it is easy to see that (2.1) will be suppressed by an additional factor of m_b^2/m_H^2 , because the vector boson Higgs decay modes $H^{SM} \rightarrow W^+ W^- (Z Z)$ will be kinematically available and become dominant. But at the same time the ratio m_H^4/m_b^2 is replaced by m_t^4/m_b^2 . Hence,

$$BR(H^{SM} \rightarrow b \bar{s}) \sim \left(\frac{|V_{ts}|}{16\pi^2} \right)^2 \alpha_W G_F \left(\frac{m_t^4}{m_H^2} \right) \lesssim 10^{-10} \quad (\text{for } m_H > m_t). \quad (2.2)$$

In the numerical evaluation we assumed a mass range where the ratio $m_H/m_t > 1$ is of order one as this provides an upper bound. In both cases (2.1) and (2.2) the branching ratios into bottom quark are much larger than the Higgs boson FCNC branching ratio into top quark in the SM [34]. However, even in the case (2.1) it is still too small to have a chance for detection in the LHC. It is clear that unless new physics comes to play the process $H^{SM} \rightarrow b \bar{s}$ (and of course $H^{SM} \rightarrow \bar{b} s$) will remain virtually invisible. Nonetheless the result (2.1) is not too far from being potentially detectable, and one might hope that it should not be too difficult for the new physics to boost it up to the observable level.

Consider how to estimate the potentially augmented rates for the MSSM processes (1.1), if only within a similarly crude approximation as above. Because of the strong FCNC gluino couplings mentioned in Section 1 and the $\tan \beta$ -enhancement inherent to the MSSM Yukawa couplings (see Ref. [30, 31] for details), we may expect several orders of magnitude increase of the branching ratios (1.2) as compared to the previous SM result. A naive approach might however go too far. For instance, one could look at the general structure of the couplings and venture an enhancement factor typically of order $(\alpha_s/\alpha_W)^2 \tan^2 \beta |\delta_{23}/V_{ts}|^2$, which for $\delta_{23} \lesssim 1$ and $\tan \beta > 30$ could easily rocket the SM result some 5 – 6 orders of magnitude higher, bringing perhaps one of the MSSM rates (1.2) to the “scandalous” level of 10% or more. But of course only a more elaborated calculation, assisted by a judicious consideration of the various experimental restrictions,

²See Ref. [34] for details on similar estimates, like that of $BR(H^{SM} \rightarrow t \bar{c})$.

³To our knowledge, the first evaluation of the SM branching ratio was performed in [40], however no detailed analysis of it exists in the literature. It is natural to clarify this value before jumping to evaluate the possible non-SM contributions. For the details, see Ref. [41].

can provide a reliable result. As we shall see, a thorough analysis generally disproves the latter overestimate.

The detailed computation of the SUSY-QCD one-loop partial decay widths $\Gamma(h \rightarrow qq')$ in (1.2) within the MSSM follows closely that of $\Gamma(t \rightarrow ch)$ (see Ref. [30, 31]). The rather cumbersome analytical expressions will not be listed here as they are a straightforward adaptation of those presented in the aforementioned references. However, there are a few subtleties that need to be pointed out. One of them is related to the calculation of the total widths $\Gamma(h \rightarrow X)$ for the three Higgs bosons $h = h^0, H^0, A^0$ in the MSSM. As long as $\Gamma(h \rightarrow qq')$ in the numerator of Eq. (1.2) is computed at leading order, the denominator has to be computed also at leading order, otherwise an artificial enhancement of $B(h \rightarrow qq')$ can be generated. For example, including the next-to-leading (NLO) order QCD corrections to $\Gamma(h \rightarrow b\bar{b})$ reduces the decay width by a significant amount [42–46]. Then, to be consistent, the NLO (two-loop) contributions to $\Gamma(h \rightarrow qq')$ should also be included. Similarly, the one-loop SUSY-QCD corrections to $\Gamma(h \rightarrow b\bar{b})$ can be very large and negative [47], which would enhance $B(h \rightarrow qq')$. At the same time these corrections also contribute to $\Gamma(h \rightarrow qq')$, such that contributions to the numerator and denominator of Eq. (1.2) compensate (at least partially) each other. Therefore the same order of perturbation theory must be used in both partial decay widths entering the observable $B(h \rightarrow qq')$ to obtain a consistent result. By the same token, using running masses in the numerator of (1.2) is mandatory, if they are used in the denominator. Last, but not least, consistency with the experimental bounds on related observables should also be taken into account. In this respect an essential role is played by the constraints on the FCNC couplings from the measured value of $B(b \rightarrow s\gamma)$. They must be included in this kind of analysis, if we aim at a realistic estimate of the maximal rates expected for the FCNC processes (1.1) in the MSSM. In our calculation we have used the full one-loop MSSM contributions to $B(b \rightarrow s\gamma)$ as given in [48]⁴.

Let us now summarize the conditions under which we have performed the computation and the approximations and assumptions made in the present analysis:

- We include the full one-loop SUSY-QCD contributions to the partial decay widths $\Gamma(h \rightarrow qq')$ in (1.2).
- We assume that FCNC mixing terms appear only in the LH-chiral sector of the squark mixing matrix. This is the most natural assumption, and, moreover, it was proven in Ref. [30, 31] that the presence of FCNC terms in the RH-chiral sector enhances the partial widths by a factor two at most – not an order of magnitude.
- The Higgs bosons total decay widths $\Gamma(h \rightarrow X)$ are computed at leading order, including all the relevant channels: $\Gamma(h \rightarrow f\bar{f}, ZZ, W^+W^-, gg)$. The off-shell decays $\Gamma(h \rightarrow ZZ^*, W^\pm W^{\mp*})$ have also been included. The one-loop decay rate $\Gamma(h \rightarrow gg)$ has been taken from [49] and the off-shell decay partial widths have been computed explicitly and found perfect agreement with the old literature on the subject [50].

⁴Ref. [48] contains a partial two-loop computation of $B(b \rightarrow s\gamma)$, but only the one-loop contributions have been used for the present work.

We have verified that some of the aforementioned higher order decays are essential to consistently compute the total decay width of $\Gamma(h^0 \rightarrow X)$ in certain regions of the parameter space where the maximization procedure probes domains in which some (usually leading) two-body processes become greatly diminished. We have checked that our implementation of the various Higgs boson decay rates is consistent with the results of `HDECAY` [51]. However, care must be exercised if using the full-fledged result from `HDECAY`. For example, it would be inconsistent, and numerically significant, to compute the total widths $\Gamma(h \rightarrow X)$ with this program and at the same time to compute the SUSY-QCD one-loop partial widths $\Gamma(h \rightarrow qq')$ without including the leading conventional QCD effects through e.g. the running quark masses.

- The Higgs sector parameters (masses and CP-even mixing angle α) have been treated using the leading m_t and $m_b \tan \beta$ approximation to the one-loop result [52–55]. For comparison, we also perform the analysis using the tree-level approximation.
- We include the constraints on the MSSM parameter space from $B(b \rightarrow s\gamma)$. We adopt $B(b \rightarrow s\gamma) = (2.1 - 4.5) \times 10^{-4}$ as the experimentally allowed range within three standard deviations [1]. Only the SUSY-QCD contributions induced from tree-level FCNCs are considered in the present work.

Running quark masses ($m_q(Q)$) and strong coupling constants ($\alpha_s(Q)$) are used throughout. More details are given below, as necessary.

3. Full one-loop SUSY-QCD calculation: Numerical analysis

Given the setup described in Section 2, we have performed a systematic scan of the MSSM parameter space with the following restrictions:

$$\begin{aligned}
 \delta_{23} &< 10^{-0.09} \simeq 0.81 \\
 A_b &= -1500 \cdots 1500 \text{ GeV} \\
 \mu &= -1000 \cdots 1000 \text{ GeV} \\
 m_{\tilde{q}} &= 150 \cdots 1000 \text{ GeV}
 \end{aligned}
 \tag{3.1}$$

and the following fixed parameters:

$$\begin{aligned}
 \tan \beta &= 50 \\
 m_{\tilde{b}_L} &= m_{\tilde{b}_R} = m_{\tilde{t}_R} = m_{\tilde{g}} = m_{\tilde{q}} \\
 A_t &= -300 \text{ GeV} .
 \end{aligned}
 \tag{3.2}$$

Here $m_{\tilde{b}_{L,R}}$ are the left-chiral and right-chiral bottom-squark soft-SUSY-breaking mass parameters, and $m_{\tilde{q}}$ is a common mass for the strange- and down-squark left- and right-chiral soft SUSY-breaking mass parameters. Following the same notation as in [30], the parameter δ_{23} represents the mixing between the second and third generation squarks. Let us recall its definition:

$$\delta_{23} \equiv \frac{m_{\tilde{b}_L}^2}{m_{\tilde{b}_L} m_{\tilde{s}_L}},
 \tag{3.3}$$

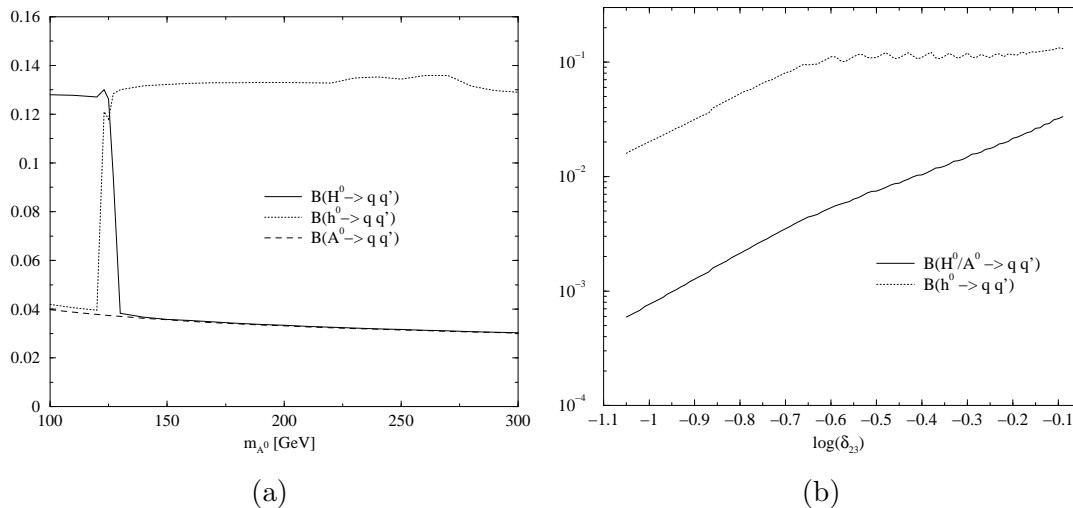


Figure 1: Maximum SUSY-QCD contributions to $B(h \rightarrow qq')$, Eq. (1.2), as a function of **a)** m_{A^0} and **b)** δ_{23} for $m_{A^0} = 200$ GeV.

Particle	H^0	h^0	A^0
$B(h \rightarrow qq')$	3.3×10^{-2}	1.3×10^{-1}	3.3×10^{-2}
$\Gamma(h \rightarrow X)$	11.0 GeV	1.6×10^{-3} GeV	11.3 GeV
δ_{23}	$10^{-0.09}$	$10^{-0.1}$	$10^{-0.09}$
$m_{\tilde{q}}$	975 GeV	975 GeV	975 GeV
A_b	1500 GeV	730 GeV	1290 GeV
μ	980 GeV	1000 GeV	980 GeV
$B(b \rightarrow s\gamma)$	4.42×10^{-4}	4.23×10^{-4}	4.50×10^{-4}

Table 1: Maximum values of $B(h \rightarrow qq')$ and corresponding SUSY parameters for $m_{A^0} = 200$ GeV.

$m_{b_L \bar{s}_L}^2$ being the non-diagonal term in the squark mass matrix squared mixing the second and third generation left-chiral squarks. The parameter δ_{23} is a fundamental parameter in our analysis as it determines the strength of the tree-level FCNC interactions induced by the supersymmetric strong interactions, which are then transferred to the loop diagrams of the Higgs boson FCNC decays (1.1).

The result of the scan is depicted in Fig. 1. To be specific: Fig. 1a shows the maximum value $B^{\max}(h \rightarrow qq')$ of the FCNC decay rate (1.2) under study as a function of m_{A^0} ; Fig. 1b displays $B^{\max}(h \rightarrow qq')$ as a function of the mixing parameter δ_{23} for $m_{A^0} = 200$ GeV. Looking at Fig. 1 three facts strike the eye immediately : i) the maximum is huge (13%!) for a FCNC rate, actually it is as big as initially guessed from the rough estimates made in Section 2; ii) very large values of δ_{23} are allowed; iii) the maximum rate is independent of the pseudo-scalar Higgs boson mass m_{A^0} . We will now analyze facts ii) and iii) in turn, and will establish their incidence on fact i). For further reference, in Table 1 we show the numerical values of $B^{\max}(h \rightarrow qq')$ together with the parameters which maximize the rates for $m_{A^0} = 200$ GeV.

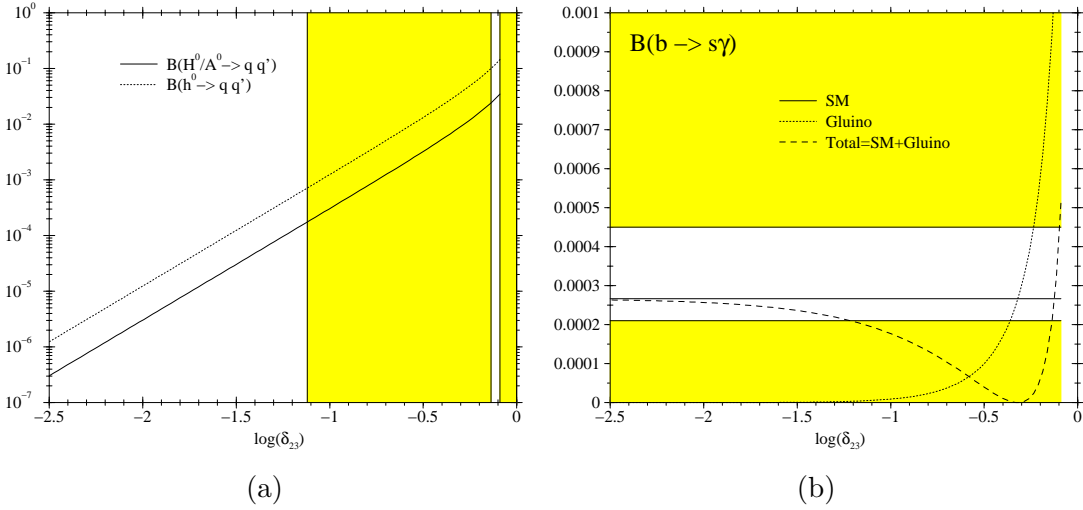


Figure 2: $B(h \rightarrow qq')$ and $B(b \rightarrow s\gamma)$ as a function of δ_{23} for the parameters that maximize $B(h^0 \rightarrow qq')$ in Table 1. The shaded region is excluded experimentally.

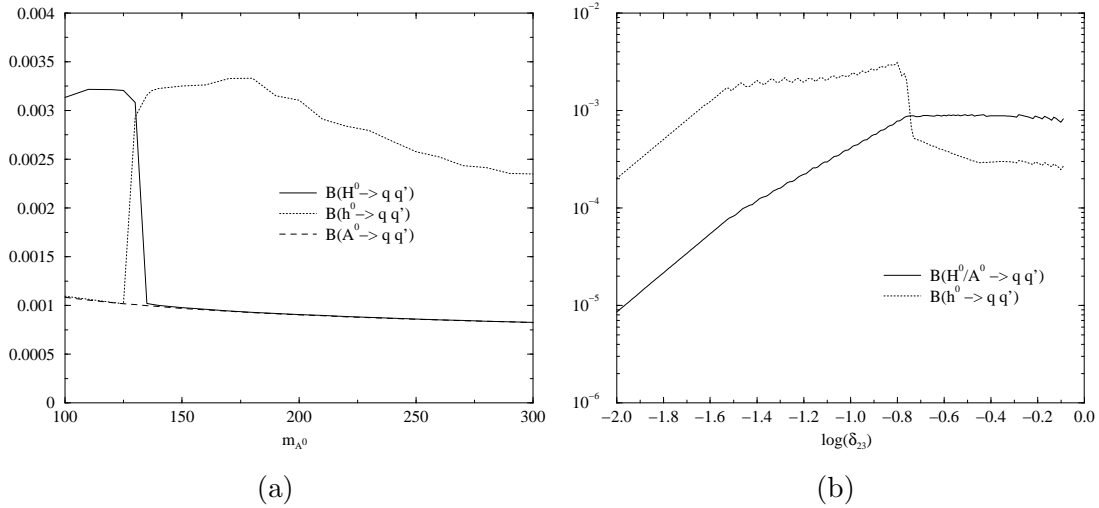


Figure 3: Maximum value of the SUSY-QCD contributions to $B(h \rightarrow qq')$ as a function of **a)** m_{A^0} and **b)** δ_{23} for $m_{A^0} = 200$ GeV, for the scenario excluding the *window* regions.

One would expect that a large value of δ_{23} should induce a large gluino contribution to $B(b \rightarrow s\gamma)$. In fact it does! However our automatic scanning process picks up the corners of parameter space where the gluino contribution alone is much larger than the SM contribution, but opposite in sign, such that both contributions destroy themselves partially leaving a result in accordance with the experimental constraints. We examine this behaviour in Fig. 2, where we show the values of $B(h \rightarrow qq')$ together with $B(b \rightarrow s\gamma)$ as a function of δ_{23} for the parameters which maximize the FCNC rate of the lightest CP-even state h^0 in Table 1. We see that, for small values of δ_{23} , the gluino contribution to $B(b \rightarrow s\gamma)$ is small, and the total $B(b \rightarrow s\gamma)$ prediction is close to the SM expectation. In contrast, as δ_{23} steadily grows, $B(b \rightarrow s\gamma)$ decreases fast (meaning a dramatic cancellation between the two contributions) until reaching a point where $B(b \rightarrow s\gamma) = 0$. From there on

Particle	H^0	h^0	A^0
$B(h \rightarrow q q')$	9.1×10^{-4}	3.1×10^{-3}	9.1×10^{-4}
$\Gamma(h \rightarrow X)$	11.2 GeV	1.4×10^{-3} GeV	11.3 GeV
δ_{23}	$10^{-0.43}$	$10^{-0.8}$	$10^{-0.43}$
$m_{\tilde{q}}$	1000 GeV	975 GeV	1000 GeV
A_b	-1500 GeV	-1500 GeV	-1500 GeV
μ	-460 GeV	-1000 GeV	-460 GeV
$B(b \rightarrow s\gamma)$	4.49×10^{-4}	4.48×10^{-4}	4.49×10^{-4}

Table 2: Maximum values of $B(h \rightarrow q q')$ and corresponding SUSY parameters for $m_{A^0} = 200$ GeV excluding the *window* region.

it starts to grow with a large slope, and in its race eventually crosses the allowed $B(b \rightarrow s\gamma)$ region. The crossing is very fast, and so rather ephemeral in the δ_{23} variable, and it leads to the appearance of a narrow allowed *window* at large δ_{23} values, see Fig. 2a. We would regard the choice of this window as a fine-tuning of parameters, hence unnatural. For this reason we reexamine the $B(h \rightarrow q q')$ ratio by performing a new scan of the MSSM parameter space in which we exclude the fine-tuned (or *window*) region. The result for $m_{A^0} = 200$ GeV can be seen in Table 2 and Fig. 3. This time we see that the maximum values of $B(h \rightarrow q q')$ are obtained for much lower values of δ_{23} , and the maximum rates have decreased more than one order of magnitude with respect to Table 1, reaching the level of few per mil. These FCNC rates can still be regarded as fantastically large. Had we included the SUSY-EW contributions to $B(b \rightarrow s\gamma)$, further cancellations might have occurred between the SUSY-EW and the SUSY-QCD amplitudes. Even more: since each contribution depends on a separate set of parameters, one would be able to find a set of parameters in the SUSY-EW sector which creates an amplitude that compensates the SUSY-QCD contributions for almost any point of the SUSY-QCD parameter space [41]. But of course this would be only at the price of performing some fine tuning, which is not the approach we want to follow here.

On the other hand further contributions to $B(b \rightarrow s\gamma)$ might exist. In the most general MSSM, flavor-changing interactions for the right-chiral squarks (δ_{23RR}), and mixing left- and right-chiral squarks (δ_{23LR}) can be introduced. The latter can produce significant contributions to $B(b \rightarrow s\gamma)$, changing the allowed parameter space. The introduction of δ_{23LR} can produce two possible outcomes: First, in certain regions of the parameter space, the contributions of δ_{23LR} and δ_{23} are of the same sign, enhancing each other. In this situation, the maximum allowed value of δ_{23} is obtained for $\delta_{23LR} = 0$. Second, in other regions of the parameter space the two contributions would compensate each other, producing an overall value of $B(b \rightarrow s\gamma)$ in accordance with experimental constraints, even though each contribution would be much larger. Again, we would regard these compensations as unnatural, and would discard that region of the parameter space. In the following we will require that the SUSY-QCD contributions induced by δ_{23} do not compensate the SM ones to give an acceptable value of $B(b \rightarrow s\gamma)$; this is equivalent to the condition that the SUSY-QCD

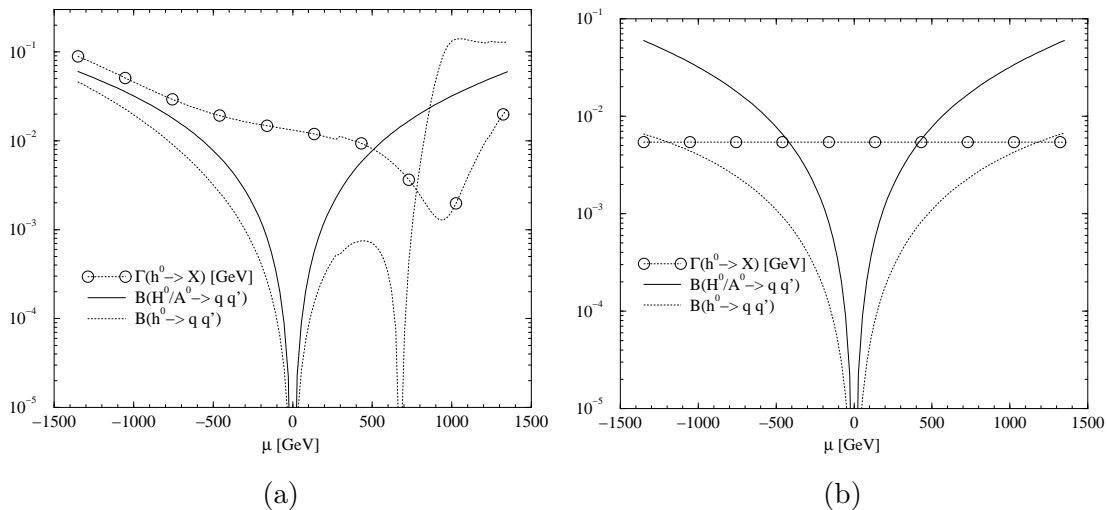


Figure 4: $B(h \rightarrow qq')$ and $\Gamma(h^0 \rightarrow X)$ (in GeV) as a function of μ for **a)** one-loop α angle; **b)** tree-level α angle, and for the parameters that maximize $B(h^0 \rightarrow qq')$ in Table 1. The H^0 and A^0 curves coincide. The $B(b \rightarrow s\gamma)$ constraint is not shown.

amplitude represents a small contribution to the total $B(b \rightarrow s\gamma)$ value, and is therefore independent of the inclusion of the other contributions (SUSY-EW, δ_{23LR}).⁵

We turn now our view to the second fact, namely the independence of the maximum rates with respect to m_{A^0} . We will show that it also plays a central role as to the enhancement of $B(h \rightarrow qq')$. Actually, a good hint is given by the small values of the lightest Higgs boson decay width in Tables 1 and 2, $\Gamma(h^0 \rightarrow X) \sim 2 \times 10^{-3}$ GeV. The maximization process of $B(h^0 \rightarrow qq')$ does not only find the parameters for which $\Gamma(h^0 \rightarrow qq')$ is maximum, but also the parameters for which $\Gamma(h^0 \rightarrow X)$ is minimum. Specifically, since $\Gamma(h^0 \rightarrow b\bar{b})$ is the dominant decay channel of h^0 for large $\tan\beta$, the maximum of $B(h^0 \rightarrow qq')$ is produced in the parameter range of the so-called *small α_{eff} scenario* [56], that is, a parameter range where the radiative corrections make the CP-even Higgs boson mixing angle α vanish (or very small), such that the leading partial decay width $\Gamma(h^0 \rightarrow b\bar{b})$ is strongly suppressed. The consequences of this scenario have been extensively studied in Ref. [57]. As advertised in Section 2, the possibility that the maximization process explores these regions of the parameter space is the reason why the leading higher order decay channels, and also the leading three-body decay modes have to be taken into account in the computation of the total width.

In Fig. 4 we plot the value of the various branching ratios $B(h \rightarrow qq')$ and of the total width of the lightest CP-even Higgs boson, $\Gamma(h^0 \rightarrow X)$, as a function of the higgsino mass parameter μ , the rest of the parameters being those of the third column of Table 1, i.e. the ones that maximize the branching ratio $B(h^0 \rightarrow qq')$. Fig. 4a shows that $\Gamma(h^0 \rightarrow X)$ has a deep minimum in the range of μ corresponding to the maximum of $B(h^0 \rightarrow qq')$, which reaches the level of a few percent. If, instead of using the radiatively corrected α

⁵The analysis of Ref. [36] follows the opposite approach, that is: to find the fine-tuning conditions imposed by low energy data that allow for the largest possible value of the FCNC parameters.

Particle	H^0	h^0	A^0
$B(h \rightarrow qq')$	9.0×10^{-4}	1.3×10^{-4}	9.0×10^{-4}
$\Gamma(h \rightarrow X)$	11.3 GeV	5.4×10^{-3} GeV	11.3 GeV
δ_{23}	$10^{-0.43}$	$10^{-0.28}$	$10^{-0.43}$
$m_{\tilde{q}}$	1000 GeV	1000 GeV	1000 GeV
A_b	-1500 GeV	-1500 GeV	-1500 GeV
μ	-460 GeV	-310 GeV	-460 GeV
$B(b \rightarrow s\gamma)$	4.49×10^{-4}	4.50×10^{-4}	4.49×10^{-4}

Table 3: Maximum values of $B(h \rightarrow qq')$ and corresponding SUSY parameters for $m_{A^0} = 200$ GeV, using the tree-level expressions for the Higgs sector, and excluding the *window* region.

value we use the tree-level expression, we obtain the result shown in Fig. 4b. Here the total decay width of the Higgs boson is independent of μ , and $B(h \rightarrow qq')$ does not show any peak. Actually in this case the branching ratio for h^0 becomes smaller than that of H^0 and A^0 for all μ . The maximization procedure in Fig. 1 selects for each value of m_{A^0} the MSSM parameters corresponding to the small α_{eff} scenario for that specific value of m_{A^0} . Of course, this discussion regarding the h^0 channels for large values of m_{A^0} has a correspondence with the H^0 channel for low values⁶ of m_{A^0} .

As indicated in Section 2, we have used a one-loop approximation for the Higgs sector [52–55], instead of the more sophisticated complete two-loop result present in the literature [58, 59]. However, we should stress that the exact MSSM parameters at which the small α_{eff} scenario is realized are not important for the sake of the present analysis. All that matters is that some portion of the parameter space exists, for which $\Gamma(h^0 \rightarrow b\bar{b})$ is strongly suppressed, but $\Gamma(h^0 \rightarrow qq')$ is not.

To compare the maximum value of $B(h^0 \rightarrow qq')$ obtained with and without the small α_{eff} scenario, we have performed the maximization procedure using the tree-level expressions for the Higgs sector parameters. The result is shown in Table 3 and Fig. 5. In this case $B(h^0 \rightarrow qq')$ is reduced by a sizeable factor of $\gtrsim 20$ with respect to Table 2, whereby the h^0 rate descends about an order of magnitude below that of the H^0/A^0 channels which remain basically unchanged. Notice also that $\Gamma(h^0 \rightarrow X)$ is larger than in previous tables. In spite of the reduction, achieving a FCNC ratio $B(h^0 \rightarrow qq') \sim 1.3 \times 10^{-4}$ is a remarkable result, three orders of magnitude larger than the maximum SM rate (2.1), and only one order of magnitude below the rare decay $B(h^0 \rightarrow \gamma\gamma) \sim 10^{-3}$. Also worth noticing in Fig. 5b (and Fig. 3b) is the fact that $B^{\max}(h \rightarrow qq')$ is essentially flat in δ_{23} in the upper range down to $\delta_{23} \sim 10^{-0.8} \simeq 0.16$. The reason lies in the correlation between $B(h \rightarrow qq')$ and $B(b \rightarrow s\gamma)$. In order to comply with the (non-fine-tuned) value of $B(b \rightarrow s\gamma)$ for large δ_{23} , the absolute value of the μ parameter must be small. When δ_{23} decreases, $|\mu|$ can grow to larger values, leaving the overall maximum rates $B^{\max}(h \rightarrow qq')$ effectively unchanged (see Eq. (3.5) below).

⁶Large or low values here means $m_{A^0} > m_{h^0}^{\max}$ or $m_{A^0} < m_{h^0}^{\max}$, i.e. above or below the maximum possible value for the mass of the lightest Higgs boson h^0 , respectively.

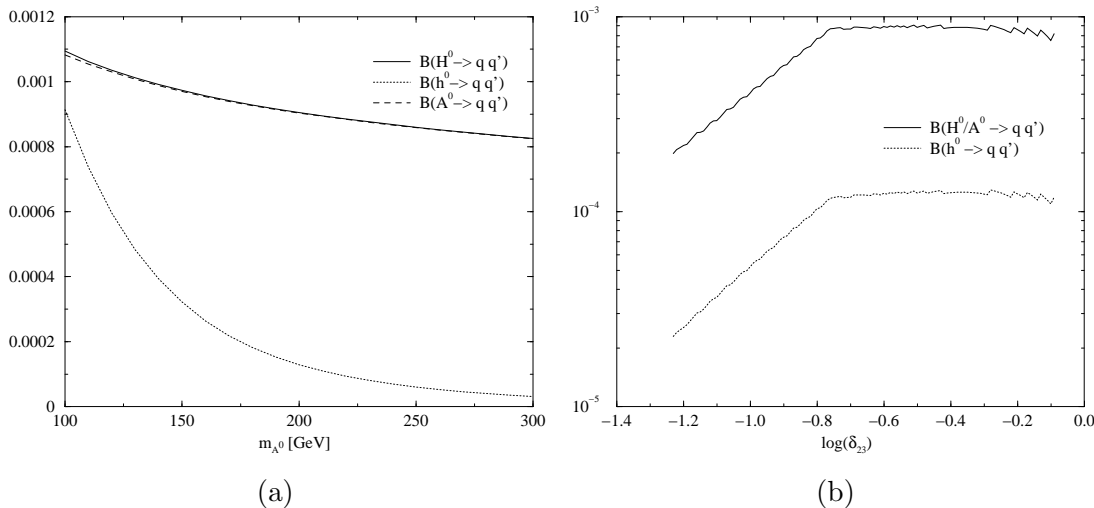


Figure 5: Maximum value of the SUSY-QCD contributions to $B(h \rightarrow qq')$ as a function of **a)** m_{A^0} and **b)** δ_{23} , for $m_{A^0} = 200$ GeV and for the scenario excluding the *window* region and using the tree-level expressions for the Higgs sector parameters.

The maximization process selects a squark mass scale in the vicinity of the maximum values used in the scanning procedure. We should point out, however, that the same order of magnitude for $B(h \rightarrow qq')$ could be obtained with a much lower squark mass scale. In this case the lighter squark masses induce a much larger $B(b \rightarrow s\gamma)$ value, and δ_{23} is much more constrained. For example, if we perform a scan in the parameter space (3.1), but fixing the squark mass scale to be $m_{\tilde{q}} < 500$ GeV, we obtain the following values for the maximal branching ratios for $m_{A^0} = 200$ GeV:

$$B^{\max}(h^0 \rightarrow qq') = 1.4 \times 10^{-5}, \quad B^{\max}(H^0/A^0 \rightarrow qq') = 9.2 \times 10^{-5}, \quad (3.4)$$

with $\delta_{23} \sim 10^{-0.6}$, $\mu \sim -110$ GeV, and we have limited ourselves to the scenario avoiding the *window* regions and using the tree-level expression for the Higgs sector parameters. These numbers have to be compared with Table 3.

The reason behind this *scale independence* admits an explanation in terms of an effective Lagrangian approach [41], in which one can estimate the leading effective coupling to behave approximately as:

$$g_{hb\bar{s}} \simeq \frac{gm_b}{\sqrt{2}M_W \cos\beta} \frac{2\alpha_s}{3\pi} \delta_{23} \frac{-\mu m_{\tilde{q}}}{M_{SUSY}^2} \begin{cases} \sin(\beta - \alpha) & (H^0) \\ \cos(\beta - \alpha) & (h^0) \\ \sin(2\beta) & (A^0) \end{cases}. \quad (3.5)$$

Aside from ensuring (at least) a partial SUSY scale independence of the leading terms, this expression also shows that $B(h \rightarrow qq')$ has a weak dependence on the soft-SUSY-breaking trilinear coupling A_b . The observed situation is similar to the flavor-conserving $hb\bar{b}$ interactions, where the cancellation of the A_b terms at leading order has been recently proven [60]. It also shows that the leading non-decoupling SUSY contributions to $\Gamma(h^0 \rightarrow qq')$ eventually fade out as the decoupling limit of the Higgs sector is approached: $\cos(\beta -$

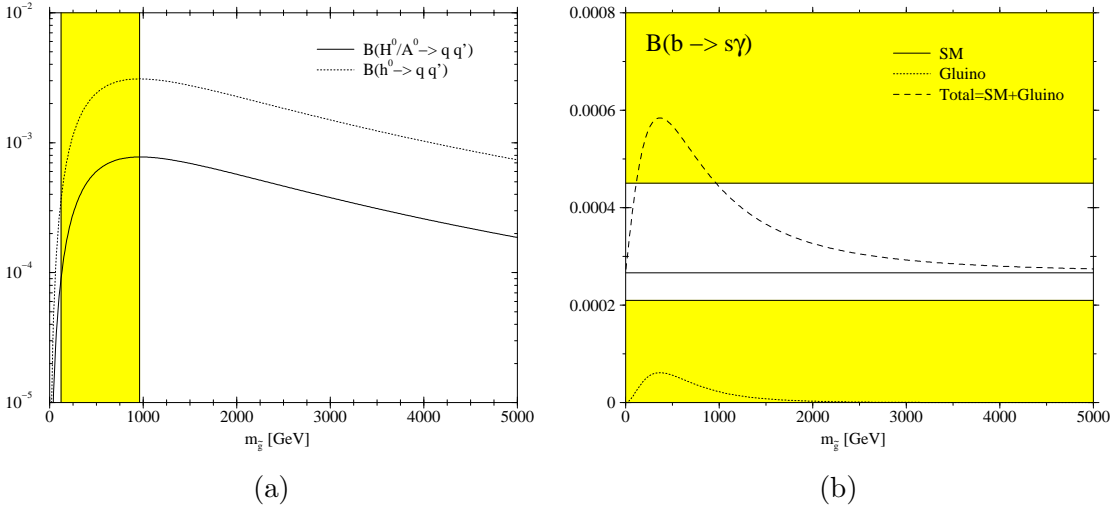


Figure 6: $B(h \rightarrow qq')$ and $B(b \rightarrow s\gamma)$ as a function of $m_{\tilde{g}}$ for the parameters that maximize $B(h^0 \rightarrow b\bar{s})$ excluding the window region (see third column of Table 2). The shaded region is excluded experimentally.

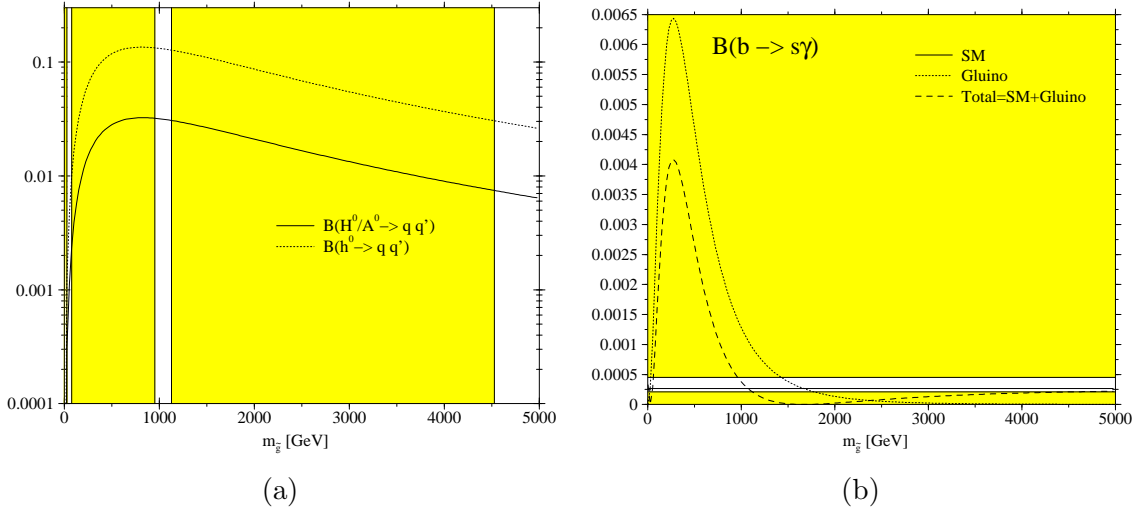


Figure 7: As in Fig. 6, but including the window region. The remaining parameters are fixed as in the third column of Table 1.

$\alpha) \rightarrow 0$. We have found (using the tree-level expression for α) that the non-leading (SUSY-decoupling) contributions to $\Gamma(h^0 \rightarrow qq')$ dominate for $m_{A^0} \gtrsim 450$ GeV, inducing a value $\Gamma^{\max}(h^0 \rightarrow qq') \sim 1.2 \times 10^{-5}$, with $\delta_{23} \sim 10^{-1}$, $\mu \sim 1000$ GeV. Full details on the effective Lagrangian approach, and its application to further refine these calculations, will be given in a forthcoming publication [41].

We further investigate the role of the scale of SUSY masses, and the fine-tuning behaviour in Figs. 6 and 7. In these figures we give up the equality $m_{\tilde{g}} = m_{\tilde{q}}$ (3.2), the squark masses are fixed at the values stated in Tables 2 and 1 respectively. Fig. 6 shows the values of $B(h \rightarrow qq')$ for the three Higgs decays and of $B(b \rightarrow s\gamma)$ as a function of the gluino

Particle	H^0		h^0		A^0	
	Γ (GeV)	$B(h \rightarrow qq')$	Γ (GeV)	$B(h \rightarrow qq')$	Γ (GeV)	$B(h \rightarrow qq')$
small- α_{eff} <i>window</i>	11.0	3.3×10^{-2}	1.6×10^{-3}	1.3×10^{-1}	11.3	3.3×10^{-2}
tree-Higgs <i>window</i>	11.3	3.3×10^{-2}	5.4×10^{-3}	4.3×10^{-3}	11.3	3.3×10^{-2}
small- α_{eff} no- <i>window</i>	11.2	9.1×10^{-4}	1.4×10^{-3}	3.1×10^{-3}	11.3	9.0×10^{-4}
tree-Higgs no- <i>window</i>	11.3	9.1×10^{-4}	5.4×10^{-3}	1.3×10^{-4}	11.3	9.0×10^{-4}
$\tan \beta = 5$	0.11	2.0×10^{-3}	6.0×10^{-3}	1.7×10^{-4}	0.11	2.1×10^{-3}
$\tan \beta = 5$ tree Higgs	0.12	1.9×10^{-3}	4.4×10^{-3}	2.6×10^{-4}	0.11	2.1×10^{-3}
$\tan \beta = 5$ no- <i>window</i>	0.15	3.8×10^{-4}	9.7×10^{-3}	1.1×10^{-4}	0.11	5.1×10^{-4}

Table 4: Maximum values of $B(h \rightarrow qq')$ and corresponding $\Gamma(h \rightarrow X)$ for the different scenarios studied in this work.

mass for the parameters that maximize $B(h^0 \rightarrow qq')$ when the *window* regions are excluded (third column of Table 2). Here we see that, while the gluino contribution to $B(b \rightarrow s\gamma)$ decouples *fast* as a function of $m_{\tilde{g}}$, its contribution to $B(h \rightarrow qq')$ is fairly sustained. Indeed, between $m_{\tilde{g}} = 1$ TeV and $m_{\tilde{g}} = 5$ TeV $B(h^0 \rightarrow qq')$ decreases only by a factor $\sim 1/4$, while the gluino contribution to $B(b \rightarrow s\gamma)$ becomes negligible at $m_{\tilde{g}} = 5$ TeV and we recover the SM prediction. As a consequence, the maximum rates $B(h \rightarrow qq')$ that we have found are robust, in the sense that further theoretical refinements and experimental results that change the allowed range of $B(b \rightarrow s\gamma)$ can easily be compensated for by a slight increase of the gluino mass ($m_{\tilde{g}}$), which would leave the prediction for $B(h \rightarrow qq')$ essentially unchanged. We note in Fig. 7 the corresponding behaviour of $B(h^0 \rightarrow qq')$ and $B(b \rightarrow s\gamma)$ in the presence of fine-tuning, i.e. as in Table 1. In contrast to the previous case, here we observe the presence of two tiny windows in the regions $m_{\tilde{g}} = 25 - 75$ GeV and $m_{\tilde{g}} = 950 - 1125$ GeV. In the middle region $m_{\tilde{g}} = 75 - 950$ GeV, $B(b \rightarrow s\gamma)$ is one order of magnitude larger than the allowed experimental range, and in the region above $m_{\tilde{g}} = 1125$ GeV it only enters the allowed region for $m_{\tilde{g}} > 4500$ GeV. In this region $B(h^0 \rightarrow qq')$ is still large, but at the price of having a gluino five times heavier than the rest of the SUSY spectrum. This is another manifestation of the large fine-tuning that governs this region of the parameter space.

Up to this point we have used the high $\tan \beta$ value quoted in Eq. (3.2). But we have also looked at the impact of varying $\tan \beta$ on $B^{\max}(h \rightarrow qq')$. Since the latest LEP data restricts $\tan \beta \gtrsim 2.5$, we have used a moderate value of $\tan \beta = 5$. Note that, at low $\tan \beta$, the small α_{eff} scenario does not arise. As a consequence similar results are obtained using either the tree-level or one-loop expressions for the Higgs sector parameters. We find that the three branching ratios $B^{\max}(h \rightarrow qq')$ at $\tan \beta = 5$ stay in the same order

of magnitude as in the scenarios with $\tan\beta = 50$ (default case) with the tree-level Higgs sector and no-window (Cf. Table 2).

4. Remarks and conclusions

The main numbers of our analysis are put in a nutshell in Table 4, where we show the results presented previously, together with some other scenarios and the low $\tan\beta$ case. The computed maximum values of $B(h \rightarrow qq')$ must not be taken as exact numbers in practice, but order of magnitude results. The implications that can be derived from Table 4 can be synthesized as follows:

1. The SUSY-QCD contributions can enhance the maximum expectation for the FCNC decay rates $B(h \rightarrow qq')$ enormously. This is seen by comparing the results of Table 4 with the maximum value of $B(H^{SM} \rightarrow b\bar{s})$ considered in Eq. (2.1). The optimized MSSM branching ratios are at the very least 3 orders of magnitude bigger than the SM result.
2. If no special circumstances apply, that is, if no fine-tuning occurs between the parameters contributing to $B(b \rightarrow s\gamma)$ in the MSSM, and if $\Gamma(h^0 \rightarrow b\bar{b})$ is not suppressed, the maximum rates are $B^{\max}(h^0 \rightarrow qq') \simeq 1.3 \times 10^{-4}$, $B^{\max}(H^0/A^0 \rightarrow qq') \simeq 9 \times 10^{-4}$. This corresponds to the *tree-Higgs/no-window* scenario in Table 4.
3. If, however, $\Gamma(h^0 \rightarrow b\bar{b})$ is suppressed by the radiative corrections to the CP-even mixing angle α , then $B(h^0 \rightarrow qq')$ can be an order of magnitude larger: $B^{\max}(h^0 \rightarrow qq') \sim 3 \times 10^{-3}$. This corresponds to the small α_{eff} scenario, and is indicated by small- α_{eff} / *no-window* in Table 4. The FCNC branching ratio that we find for h^0 in this case should be considered as the largest possible one within the conditions of naturalness (no fine-tuning).
4. On the other hand, if fine-tuning between the gluino and the SM contributions to $B(b \rightarrow s\gamma)$ is allowed, but the small- α_{eff} scenario is not realized, then $B^{\max}(h^0 \rightarrow qq')$ grows one order of magnitude up to $B^{\max}(h^0 \rightarrow qq') \sim 4 \times 10^{-3}$, whereas $B^{\max}(H^0/A^0 \rightarrow qq') \sim 3 \times 10^{-2}$. This corresponds to the case labelled *tree-Higgs/window* in Table 4.
5. When both special conditions take place simultaneously, viz. fine-tuning in $B(b \rightarrow s\gamma)$ (triggered by a very special choice of the δ_{23} parameter in a narrow window range) and small α_{eff} scenario (independent of assumptions on δ_{23}), we reach an over-optimistic situation where $B^{\max}(h^0 \rightarrow qq')$ could reach the $\sim 10\%$ level. This is the case referred to as small- α_{eff} / *window* in Table 4.
6. If $\tan\beta$ is low/moderate, then $B^{\max}(h \rightarrow qq')$ lie in the lower range $\sim 10^{-4}$, which can grow an order or magnitude for $B^{\max}(H^0/A^0 \rightarrow qq')$ in fine-tuned scenarios (last three rows in Table 4).

Although the large FCNC rates mentioned in points 4 and 5 above seem to offer a rather tempting perspective, we will not elaborate on them any further since in our opinion the fine-tuning requirement inherent in them is too contrived. On the other hand, points 2 and 3 offer a moderate, but certainly much more realistic scenario, which in no way frustrates our hopes to potentially detect the FCNC Higgs boson decays (1.1). Indeed, in the case described in point 2, $B(h \rightarrow qq')$ can be at most of order 10^{-4} . But this is still a fairly respectable FCNC branching ratio (comparable to that of $b \rightarrow s\gamma$) and it may lead to a large number of events at a high luminosity collider [41]⁷. Moreover, if $\Gamma(h \rightarrow X)$ becomes suppressed (e.g. by realizing the small α_{eff} scenario, point 3) then $B(h^0 \rightarrow qq')$ can be enhanced by an additional order of magnitude.

Our analysis correlates the values of $B(h \rightarrow qq')$ with that of $B(b \rightarrow s\gamma)$, taking into account only the SUSY-QCD contributions due to flavour mixing parameters among the left-chiral squarks. The presence of several other competing contributions to $B(b \rightarrow s\gamma)$ alters the borders of the allowed parameter space:

- For the fine-tuned scenarios, the presence and position of the allowed *window* regions in the parameter space depends significantly on all the contributions, and therefore also does the maximum value of $B(h \rightarrow qq')$. Outside the *window* regions, the computed value of $B(b \rightarrow s\gamma)$ can only be made consistent with the experimental range, by means of a large splitting between the squark and gluino masses.
- For the non-fine-tuned scenarios, the inclusion of further contributions to $B(b \rightarrow s\gamma)$ also alters the allowed parameter space, but the condition of non-fine-tuning ensures precisely that the change in the allowed range of δ_{23} is smooth, and the corresponding change in $B^{\max}(h \rightarrow qq')$ is not dramatic.

Of course, the question immediately arises on what will happen if the data from present B -meson factories further constrains the δ_{23} parameter. In that case, we should take into account the (charged-current induced) SUSY-EW contributions to $B(h \rightarrow qq')$, which will be presented in Ref. [41] (see also [61]). However, we can advance that the SUSY-EW effects on $B^{\max}(h \rightarrow qq')$ that we find are in the ballpark of $B^{\max}(h^0 \rightarrow qq') \sim 3 \times 10^{-5}$ and $B^{\max}(H^0/A^0 \rightarrow qq') \sim 1 \times 10^{-5}$ for a non-fine-tuned scenario, while $B^{\max}(h^0 \rightarrow qq') \sim 2 \times 10^{-4}$ and $B^{\max}(H^0/A^0 \rightarrow qq') \sim 8 \times 10^{-5}$ for a fine-tuned scenario. From the analysis of Ref. [34] we expect that even with these impoverished MSSM rates the number of FCNC events of that sort should be non-negligible at the LHC.

We have already mentioned that our results disagree some orders of magnitude with recent estimates presented in the literature [35]. In fact, in our analysis we cannot accommodate a branching ratio at the level of $B(h \rightarrow qq') \sim (20 - 30)\%$ for any of the decays (1.1), as claimed by these authors. We find such values incompatible with a rigorous MSSM analysis of these decays correlated with the branching ratio of $b \rightarrow s\gamma$. Even though we have detected the existence of corners of the MSSM parameter space where a Higgs boson FCNC branching ratio can barely reach the 10% level (cf. the narrow windows in Fig. 2

⁷See e.g. Ref. [34] for a detailed analysis of the number of Higgs boson FCNC events produced at the LHC in a different situation corresponding to the general 2HDM.

and Fig. 7), we insist once more that they should be considered rather unlikely as they are associated to fine tuning of the parameters. Moreover, in contrast to these authors, we find that it is the lightest CP-even state, h^0 , the one that could have the largest FCNC branching ratio. Thus, as already advanced in Ref. [34], we believe that the authors of Ref. [35] have overestimated by a significant amount the value of $B^{\max}(h \rightarrow q q')$ for the three Higgs bosons of the MSSM.

To conclude, we have presented a first realistic estimate of the branching ratios of the Higgs boson FCNC decays (1.1) within the MSSM, assuming that the SUSY-QCD corrections can be as large as permitted by the experimental constraints on $B(b \rightarrow s\gamma)$. We have carried out a systematic and self-consistent maximization of the branching ratios (1.2) taking into account this crucial experimental constraint. At the end of the day the results that we obtain, especially for the lightest CP-even Higgs boson of the MSSM, are fairly large: $B^{\max}(h^0 \rightarrow q q') \sim 10^{-4} - 10^{-3}$. These MSSM rates turn out to be between three to four orders of magnitude larger than the maximum SM rate (2.1), but not five or six orders as naive expectations indicated. Whether this branching ratio is measurable at the LHC [8, 9] or at a high energy e^+e^- Linear Collider [10] can only be established by means of specific experimental analyses. However, on the basis of related studies in the general 2HDM [34] and from ongoing work in the MSSM [41], we can foresee that an important number of FCNC events (1.1) can be potentially collected at the LHC. They could play a complementary, if not decisive, role in the identification of low-energy Supersymmetry. In this paper we have dealt only with the maximum rates induced by the SUSY-QCD sector of the model. A more detailed analysis – including the SUSY-EW sector and the computation of the aforementioned production rates – will be presented in a forthcoming publication [41].

Acknowledgments

J.G. thanks Jörg Urban for useful discussions on $b \rightarrow s\gamma$. This collaboration is part of the network “Physics at Colliders” of the European Union under contract HPRN-CT-2000-00149. The work of S.B. has been supported in part by CICYT under project No. FPA2002-00648, and that of F.D. and J.S. by MECYT and FEDER under project FPA2001-3598. F.D. has also been supported by the fellowship 2003FI 00547 of the Generalitat de Catalunya.

References

- [1] K. Hagiwara et al. (Particle Data Group Collaboration), Phys. Rev. **D66**, 010001 (2002), <http://pdg.lbl.gov>.
- [2] S. L. Glashow, J. Iliopoulos and L. Maiani, Phys. Rev. **D2**, 1285–1292 (1970).
- [3] J. F. Gunion, H. E. Haber, G. L. Kane and S. Dawson, *The Higgs hunter’s guide*, Addison-Wesley, Menlo-Park, 1990.
- [4] H. P. Nilles, Phys. Rept. **110**, 1 (1984).
- [5] H. E. Haber and G. L. Kane, Phys. Rept. **117**, 75 (1985).

- [6] A. B. Lahanas and D. V. Nanopoulos, *Phys. Rept.* **145**, 1 (1987).
- [7] S. Ferrara, editor, *Supersymmetry*, volume 1-2, North Holland/World Scientific, Singapore, 1987.
- [8] ATLAS Collaboration, *CERN/LHCC/94-43*, Atlas Technical Design Report.
- [9] CMS Collaboration, *CERN/LHCC/94-38*, CMS Technical Proposal.
- [10] J. A. Aguilar-Saavedra et al. (ECFA/DESY LC Physics Working Group Collaboration), (2001), *hep-ph/0106315*, also available at <http://tesla.desy.de/tdr>.
- [11] M. S. Alam et al. (CLEO Collaboration), *Phys. Rev. Lett.* **74**, 2885–2889 (1995).
- [12] R. Barate et al. (ALEPH Collaboration), *Phys. Lett.* **B429**, 169–187 (1998).
- [13] S. Ahmed et al. (CLEO Collaboration), (1999), *hep-ex/9908022*.
- [14] K. Abe et al. (Belle Collaboration), *Phys. Lett.* **B511**, 151–158 (2001), *hep-ex/0103042*.
- [15] S. Chen et al. (CLEO Collaboration), *Phys. Rev. Lett.* **87**, 251807 (2001), *hep-ex/0108032*.
- [16] B. Aubert et al. (BaBar Collaboration), (2002), *hep-ex/0207076*.
- [17] M. Ciuchini, G. Degrossi, P. Gambino and G. F. Giudice, *Nucl. Phys.* **B527**, 21–43 (1998), *hep-ph/9710335*.
- [18] F. M. Borzumati and C. Greub, *Phys. Rev.* **D58**, 074004 (1998), *hep-ph/9802391*.
- [19] F. M. Borzumati and C. Greub, *Phys. Rev.* **D59**, 057501 (1999), *hep-ph/9809438*.
- [20] P. Gambino and M. Misiak, *Nucl. Phys.* **B611**, 338–366 (2001), *hep-ph/0104034*.
- [21] M. J. Duncan, *Nucl. Phys.* **B221**, 285 (1983).
- [22] F. Gabbiani, E. Gabrielli, A. Masiero and L. Silvestrini, *Nucl. Phys.* **B477**, 321–352 (1996), *hep-ph/9604387*.
- [23] M. Misiak, S. Pokorski and J. Rosiek, (1997), *hep-ph/9703442*, in “Heavy Flavours II”, eds. A.J. Buras, M. Lindner, *Advanced Series on directions in High Energy Physics*, World Scientific.
- [24] R. Barbieri and G. F. Giudice, *Phys. Lett.* **B309**, 86–90 (1993), *hep-ph/9303270*.
- [25] R. Garisto and J. N. Ng, *Phys. Lett.* **B315**, 372–378 (1993), *hep-ph/9307301*.
- [26] M. A. Diaz, *Phys. Lett.* **B322**, 207–212 (1994), *hep-ph/9311228*.
- [27] F. M. Borzumati, *Z. Phys.* **C63**, 291–308 (1994), *hep-ph/9310212*.
- [28] S. Bertolini and F. Vissani, *Z. Phys.* **C67**, 513–524 (1995), *hep-ph/9403397*.
- [29] F. Borzumati, C. Greub, T. Hurth and D. Wyler, *Phys. Rev.* **D62**, 075005 (2000), *hep-ph/9911245*.
- [30] J. Guasch and J. Solà, *Nucl. Phys.* **B562**, 3–28 (1999), *hep-ph/9906268*.
- [31] S. Béjar, J. Guasch and J. Solà, (2001), *hep-ph/0101294*, in: *Proc. of the 5th International Symposium on Radiative Corrections (RADCOR 2000)*, Carmel, California, 11-15 Sep 2000.
- [32] T. Besmer, C. Greub and T. Hurth, *Nucl. Phys.* **B609**, 359–386 (2001), *hep-ph/0105292*.
- [33] S. Béjar, J. Guasch and J. Solà, *Nucl. Phys.* **B600**, 21–38 (2001), *hep-ph/0011091*.

- [34] S. Béjar, J. Guasch and J. Solà, Nucl. Phys. **B675**, 270–288 (2003), [hep-ph/0307144](#).
- [35] A. M. Curiel, M. J. Herrero and D. Temes, Phys. Rev. **D67**, 075008 (2003), [hep-ph/0210335](#).
- [36] D. A. Demir, Phys. Lett. **B571**, 193–208 (2003), [hep-ph/0303249](#).
- [37] J. Küblbeck, M. Böhm and A. Denner, Comput. Phys. Commun. **60**, 165–180 (1990).
- [38] T. Hahn and M. Pérez-Victoria, Comput. Phys. Commun. **118**, 153 (1999), [hep-ph/9807565](#).
- [39] T. Hahn, *FeynArts 2.2*, *FormCalc* and *LoopTools* user’s guides, available from <http://www.feynarts.de>.
- [40] G. Eilam, B. Haeri and A. Soni, Phys. Rev. **D41**, 875 (1990).
- [41] S. Béjar, J. Guasch and J. Solà, in preparation.
- [42] E. Braaten and J. P. Leveille, Phys. Rev. **D22**, 715 (1980).
- [43] N. Sakai, Phys. Rev. **D22**, 2220 (1980).
- [44] T. Inami and T. Kubota, Nucl. Phys. **B179**, 171 (1981).
- [45] M. Drees and K.-i. Hikasa, Phys. Rev. **D41**, 1547 (1990).
- [46] M. Drees and K.-i. Hikasa, Phys. Lett. **B240**, 455 (1990), *Erratum, ibid.* **B262**, 497 (1991).
- [47] J. A. Coarasa, R. A. Jiménez and J. Solà, Phys. Lett. **B389**, 312–320 (1996), [hep-ph/9511402](#).
- [48] C. Bobeth, M. Misiak and J. Urban, Nucl. Phys. **B567**, 153–185 (2000), [hep-ph/9904413](#).
- [49] M. Spira, A. Djouadi, D. Graudenz and P. M. Zerwas, Nucl. Phys. **B453**, 17–82 (1995), [hep-ph/9504378](#).
- [50] W.-Y. Keung and W. J. Marciano, Phys. Rev. **D30**, 248 (1984).
- [51] A. Djouadi, J. Kalinowski and M. Spira, Comput. Phys. Commun. **108**, 56–74 (1998), [hep-ph/9704448](#).
- [52] A. Yamada, Z. Phys. **C61**, 247 (1994).
- [53] P. Chankowski, S. Pokorski and J. Rosiek, Nucl. Phys. **B423**, 437–496 (1994), [hep-ph/9303309](#).
- [54] A. Dabelstein, Z. Phys. **C67**, 495–512 (1995), [hep-ph/9409375](#).
- [55] A. Dabelstein, Nucl. Phys. **B456**, 25–56 (1995), [hep-ph/9503443](#).
- [56] M. Carena, S. Heinemeyer, C. E. M. Wagner and G. Weiglein, Eur. Phys. J. **C26**, 601–607 (2003), [hep-ph/0202167](#).
- [57] M. Carena, S. Mrenna and C. E. M. Wagner, Phys. Rev. **D62**, 055008 (2000), [hep-ph/9907422](#).
- [58] M. Carena, H. Haber, S. Heinemeyer, W. Hollik, C. Wagner and G. Weiglein, Nucl. Phys. **B580**, 29–57 (2000), [hep-ph/0001002](#).
- [59] J. R. Espinosa and R.-J. Zhang, Nucl. Phys. **B586**, 3–38 (2000), [hep-ph/0003246](#).
- [60] J. Guasch, P. Häfliger and M. Spira, Phys. Rev. **D68**, 115001 (2003), [hep-ph/0305101](#).
- [61] A. M. Curiel, M. J. Herrero, W. Hollik, F. Merz and S. Peñaranda, (2003), [hep-ph/0312135](#).